Steady state control of perforated plate extractive reactors

A. O. Ghallab, R. S. Ettouney, and M. A. El-Rifai

Chemical Engineering Department, Faculty of Engineering, Cairo University, Giza, Egypt

Abstract

Model based supervisory control of a class of extractive reactors subject to both measurable and un-measurable disturbances is addressed in the light of a previously developed steady state model. The model reflects the interaction between column hydrodynamics and the rates of mass transfer and chemical reaction. The control scheme is intended to keep a specified product composition despite feed flow rate and feed composition disturbances and to ensure that the column remains within its stable hydrodynamic range. A simple logic control function selects either the solvent rate or the feed rate as the manipulated variable. In order to cope with deviations of the system physicochemical parameters from their nominal values, model based solvent or feed flow rate set point computations are corrected through an iterative scheme.

1. Introduction

The performance of perforated plate extractive reactors is affected by possible variability of many factors. The rates of mass transfer and simultaneous chemical reaction are functions of the systems physicochemical and hydrodynamic parameters. The physicochemical properties of densities, viscosities, diffusivities, interfacial tension, and reaction rate constants are liable to fluctuations due to the presence of impurities and temperature changes. Also changes in the phase flow rates either deliberately introduced or arising as disturbances are accompanied by variations in the flow pattern resulting in changes in drop diameter, dispersed phase

holdup, and slip velocity, which together with the aforementioned physical properties are reflected on the interfacial surface area and effective reaction volume.

A wide variety of models have been proposed for describing the flow pattern in mixer settlers [El-Rifai, 1975], spray, packed, and pulsed extractive reactors. These include plug flow [El-Rifai et al., 1977], axial dispersion of the continuous phase [El Nashaie et al., 1978], mixing cells with recycle [Mjalli et al., 2004], and forward mixing led by drop size distribution [Tang et al., 2004]. Computational fluid dynamic models [Bart, 2002; Attarakih et al., 2008; Hlawitschkah and Bart, 2012] have been developed for agitated and rotating disc contactors which are characterized breakage and coalescence [Valentas and Amundson, 1966] of the droplets.

In the absence of mechanical agitation, perforated plate columns are less prone to non-uniformity of age and size of the droplet population. Reliable correlations are available for expressing drop diameter, holdup, slip velocity, pressure drops, and mass transfer coefficients in terms of the design dimensions and physicochemical properties of the system. Such correlations have been used in the validation of a computational fluid mechanics model [**Yadav and Patwardhan, 2009**] of a small column.

Online control of extractive reactions involves formulation of a suitable model of the liquid-liquid contactor and synthesis of an operating optimization scheme which usually targets a constant product composition. The steady state and dynamic characteristics of the system depend on the hydrodynamics within the contactor. The rates of mass transfer and chemical reaction are affected by non-ideal flow patterns and uncertainty of physical properties. Online identification has been suggested for control [Najim and Le Lann, 1988] of pulsed sieve plate extractors. An alternative approach uses neural networks [Chouai et al., 2000] to handle the nonlinear time varying dynamics in such columns. Previous studies on process control of Scheibel columns include the use of reduced order models [Mjalli et al., 2005a] and the suggestion of adaptive model based controller tuning schemes to deal with uncertainty in process characteristics [Mjalli et al., 2005b].

Reduced order linearized models have been also developed to express the composition dynamics [Ettouney and El-Rifai, 2011] and flow transients [Ettouney and El-Rifai, 2012] in un-agitated perforated plate columns. Inherent nonlinearities and uncertainties associated with their operation are however reflected on the control system performance. These nonlinearities are mainly attributable to the static rather than the dynamic characteristics of the system. They are due to the hydrodynamic interaction between the contacted phases and to the variability of transport, kinetic,

and equilibrium parameters. A suitable approach to tackle the control problem in such systems [Bemporad and Mosca, 1998] is to separate the dynamic stabilization problem from the nonlinear constraint fulfillment problem. Individual loop dynamics are handled by conventional linear controllers while the nonlinear steady state constraints are enforced by manipulating desired set points at a higher control level [Morari and Lee, 1999].

The present paper presents an analysis of the steady state characteristics of un-agitated perforated plate extractive reactors subject to variation in physicochemical and hydrodynamic parameters. A simple model based supervisory control scheme is suggested to cope with nonlinearities associated with changes in the feed flow rates and with variability of system parameters. The scheme involves a supervisory control computer generating set points of the feed and solvent flow rate controllers. Phase flow rate perturbations required for achieving a desired raffinate composition are computed through series expansion of the model based non-linear purification ratio-phase flow rates response surfaces. Such flow changes are adaptively modified online to cope with uncertainty of the nominal design dimensions and system physicochemical parameters.

2. The model system

The model used in this work was previously developed for analyzing the design and steady state performance of countercurrent un-agitated perforated plate extractive reactors conducting a slow first order reaction in the dispersed extract phase [Ettouney et al., 2007]. The model expresses the purification ratio (x_1/x_f) by

$$\frac{x_1}{x_f} = \frac{(p_1 - p_2)}{p_1^{N+1} - p_2^{N+1} - e^{-\beta(1+\gamma)}(p_1^N - p_2^N)} \quad (1)$$

Where N is the actual number of plates and the parameters p_1, p_2, β, and γ are dimensionless parameters which are intricately related to flow rates of both phases and the physicochemical parameters of densities, viscosities, interfacial tension, solute partition coefficient, reaction rate constant, and solute diffusivities. MatLab programs were developed for the calculation of the above system characteristics on the basis of published correlations.

3. Steady state control

3.1. Normal operation

Under normal operating conditions, the feed composition and flow rate are liable to disturbances while the solvent flow rate is the variable to be manipulated. The optimum raffinate composition is dictated by economic considerations and is the main reference input to the column control system. The above model is directly applicable in the steady state computer control of an extraction column with given constant design and physicochemical parameters. The ratio between the design value of the raffinate composition and the measured feed composition define the desired value of the purification ratio $(x_1/x_f)_D$ which together with the measured value of the feed flow rate enable the estimation of the required solvent rate through Eq. (1).

The solvent flow modulation required to achieve a given purification of the feed may be quantitatively visualized by considering a typical column with given design and physicochemical parameters. Point (A) in Fig. (1) represents the operating design conditions. If the feed flow rate is increased to (3.25×10^{-3} m^3/s) the solvent rate has to be increased up to (10.75×10^{-3} m^3/s) corresponding to point (B) in order to maintain the same purification. If the liquid flow rate remains constant but the feed composition is increased and it is desired to keep the same raffinate composition, then the purification ratio has to drop down to say (0.2) this means that the solvent rate has to be increased to (10.75×10^{-3} m^3/s), corresponding to point (C). Also, assuming that the purification ratio has to be maintained at (0.2) and the feed rate is decreased down to (2.39×10^{-3} m^3/s) the solvent rate is to be decreased down to (8.5×10^{-3} m^3/s) corresponding to point (D).

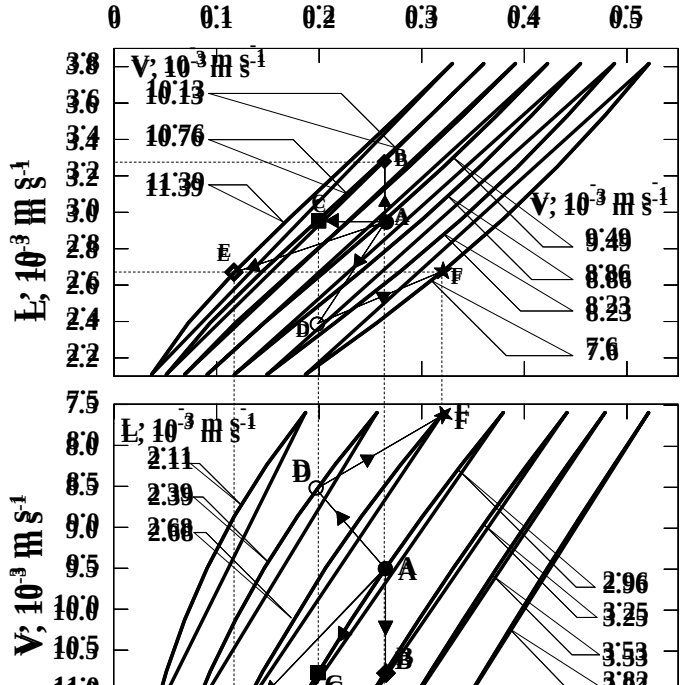

Figure (1) Modulation of phase flow rates to achieve a desired purification ratio

3.2. Limiting conditions

The flow rates of both phases have to be within the limits of the hydrodynamics stability window. Referring to Fig. (1), if the feed composition is increased up to the point where the model computed solvent flow rate exceeds the flooding rate (11.5×10^{-3} m^3/s), the solvent rate is fixed at its maximum safe level of (11.39×10^{-3} m^3/s) and the feed flow rate has to be decreased down to (2.68×10^{-3} m^3/s) as indicated by point (E). Also when the feed composition is so reduced as to correspond to a high desired value of (x_1/x_f), the solvent flow rate called for to keep the desired raffinate composition, may be below its stable operating value of (7.5×10^{-3} m^3/s). In this case V is fixed at its minimum safe value of (7.6×10^{-3} m^3/s) and the feed rate is to be increased to (2.68×10^{-3} m^3/s) as indicated by point (F).

3.3. Controller set point selection

It is clear from the above that the computer control system should respond to the hydrodynamic stability requirements by adopting two different control policies. These are to either effect a change of the solvent flow rate while the feed flow rate is left free to vary within the range of its allowable values or to fix the solvent rate at its maximum or minimum allowable limits while manipulating the feed rate through control computations. Appendix (A) outlines a simple programmable logic control scheme suitable for the selection of the variable to be manipulated.

4. Effect of physicochemical properties

The steady state control concept discussed along with Fig. (1) is suitable when the system physicochemical properties remain constant at their model values. These however, are subject to moderate changes during operation and have a direct bearing on column hydrodynamics and mass transfer performance. Temperature

and composition changes affect the system densities, viscosities, interfacial tension, diffusivities, equilibrium partition, and reaction rate. The effects of the physicochemical parameters on the purification ratio-phase flow rates response surface have been generated for a ±15% change in the above properties relative to their nominal design base case values.

The effect of changes in the values of the solute partition coefficient and of the reaction rate constant for a column with given design parameters is displayed in Figs. (2) and (3) respectively. It is seen that the response surfaces follow more or less the same form obtained for the base case. Similar trends are obtained for different values of phase viscosities, interfacial tension, and solute diffusivities but their effect is less prominent.

The steady state control system is to consider possible variations in the above parameters through an adaptive model based scheme. In this case, the model of Eq. (1) is to be simplified to enable its online application

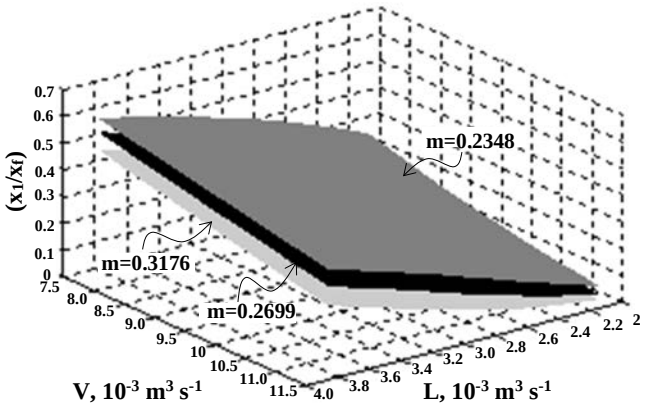

Figure (2) Effect of solute partition coefficient on the purification ratio-phase flow rates response surface

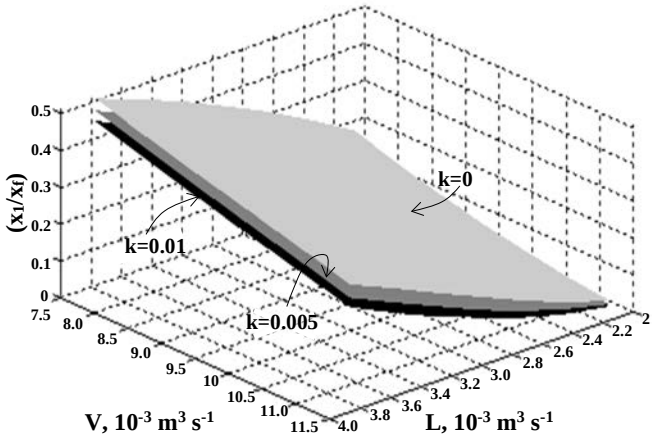

Figure (3) Effect of reaction rate constant (k, s^{-1}) on the purification ratio-phase flow rates response surface phase flow rates response surface

5. Approximation of the response surface

Since the phase flow rates are implicitly included in the right hand side of Eq. (1), its application for the generation of the relation between the purification ratio and phase flow rates involves laborious computations of the system hydrodynamics. The (x_1/x_f)-L-V relation should be simplified in order to be used in a model based control system. The rigorously generated response surfaces of the type presented in Figs. (2) and (3) may be approximated to a sixth degree polynomials in both L and

V. For a given column and nominal values of the design dimensions and constant physicochemical parameters, the response surface data may be correlated as

$$x_1 / x_f = aV^3 + bV^2 + cV + d = \psi(L, V) \qquad (2)$$

Where (a, b, c, and d) are third degree polynomials in L. Typically this approximation fits the response surface very closely with the maximum error in (x_1 / x_f) not exceeding ±0.8% at any combination of L and V.

Unlike Eq. (1), Eq. (2) is readily differentiable with respect to L and V which enables to calculate the gradients of the purification ratio response surface as $K_L = \partial(x_1/x_f)/\partial L$, and $K_V = \partial(x_1/x_f)/\partial V$ for any combination of L and V. The effect of changes in the values of the physicochemical parameters on K_L and K_V over the stable operating range of the phase flow rates has been investigated. The results indicate that as expected, K_L and K_V are sensitive to changes in phase flow rates but to a much lesser extent to ±15% change in viscosities, interfacial tension, and solute diffusivities. On the other hand, changes in the equilibrium partition coefficient and reaction rate constant have a more important effect on the obtained K_L and K_V surfaces. This is illustrated in Fig. (4) which shows that for a ±15% change in the solubility relative to a base case the deviations are more pronounced for low values of L and high values of V.

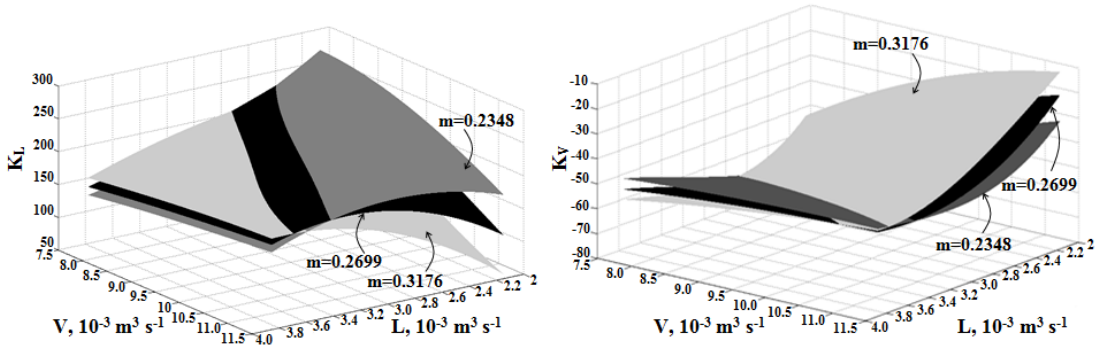

Figure (4) Effect of a ±15% change in the solvent partition coefficient on the partial derivatives K_L and K_V

6. Model based computations

In order to cope with fluctuations in the values of the physicochemical parameters, the steady state control of the raffinate composition through the manipulation of either the solvent rate or feed flow rate may resort to some sort of evolutionary operation. The model based adaptive scheme relies on first computing the values of

K_L and K_V using the model nominal values of the physicochemical and design parameters and the measured flow rates of both phases. These initial values of K_L and K_V are combinations of second degree polynomials in L and V as may be inferred from Eq. (1). They are then iteratively corrected on the basis of composition measurements as illustrated schematically in Fig. (5).

For any set of feed and solvent flow rates, an accidental decrease in the equilibrium solubility or increase in viscosity correspond to an increase of (x_1 / x_f) of the actual plant relative to the base case level. The upper curve in Fig. (5) corresponds to hypothetical actual plant measurements and the lower curve represents the model based plant performance. When the value of the feed composition x_f changes, the reference input to the control model $(x_1/x_f)_D$ also changes. Point M_1 indicates that the desired purification ratio is satisfied at the base case conditions represented by the model, while A_1 represents the actual column performance at the same flow rates. The increase in the solvent rate required to achieve the desired purification ratio in the actual plant is obtained through an iterative scheme. Such calculations are repeated over suitable time intervals depending on the column size.

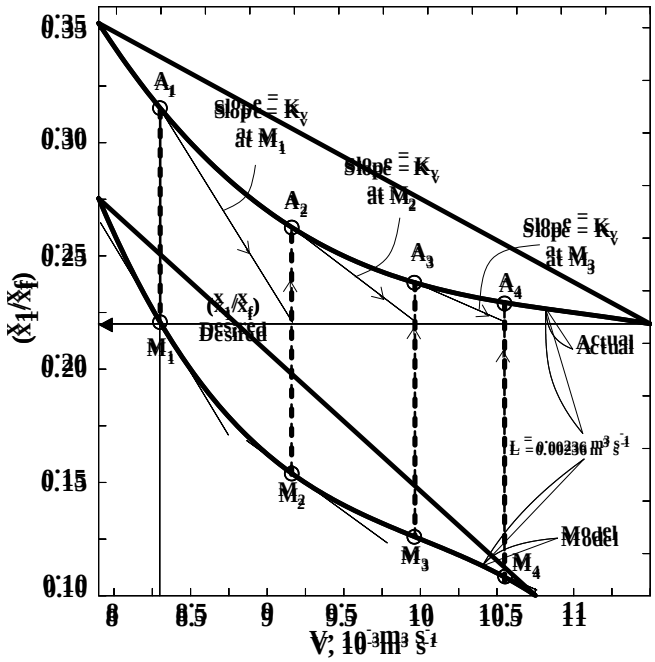

Figure (5) Adaptive iterative model based corrections of computed solvent flow rate set point

For moderate variations in the physicochemical parameters, the convergence to the desired value is quite rapid because the difference between the slopes of the actual and model cases is not as exaggerated as shown in Fig. (5). For a typical case where a 10% decrease in solubility is assumed, the purification ratio computations converge to within -8.8×10^{-4} after the first iteration and to within 10^{-5} after the third iteration. This calls for an increase of the solvent rate from 9.495×10^{-3} m^3/s to 10.349×10^{-3} m^3/s.

7. Outline of the adaptive control scheme

Fig. (6) outlines the configuration of the suggested computer control scheme for a plate column extractor. It is seen that the flow measurements are fed to both conventional flow controllers as well as the control computer. For new plants, the flow controllers of the feed and solvent rates may be integrated within the main control computer. The interface level controllers at the top and bottom of the column may also be either plant mounted or integrated within the computer.

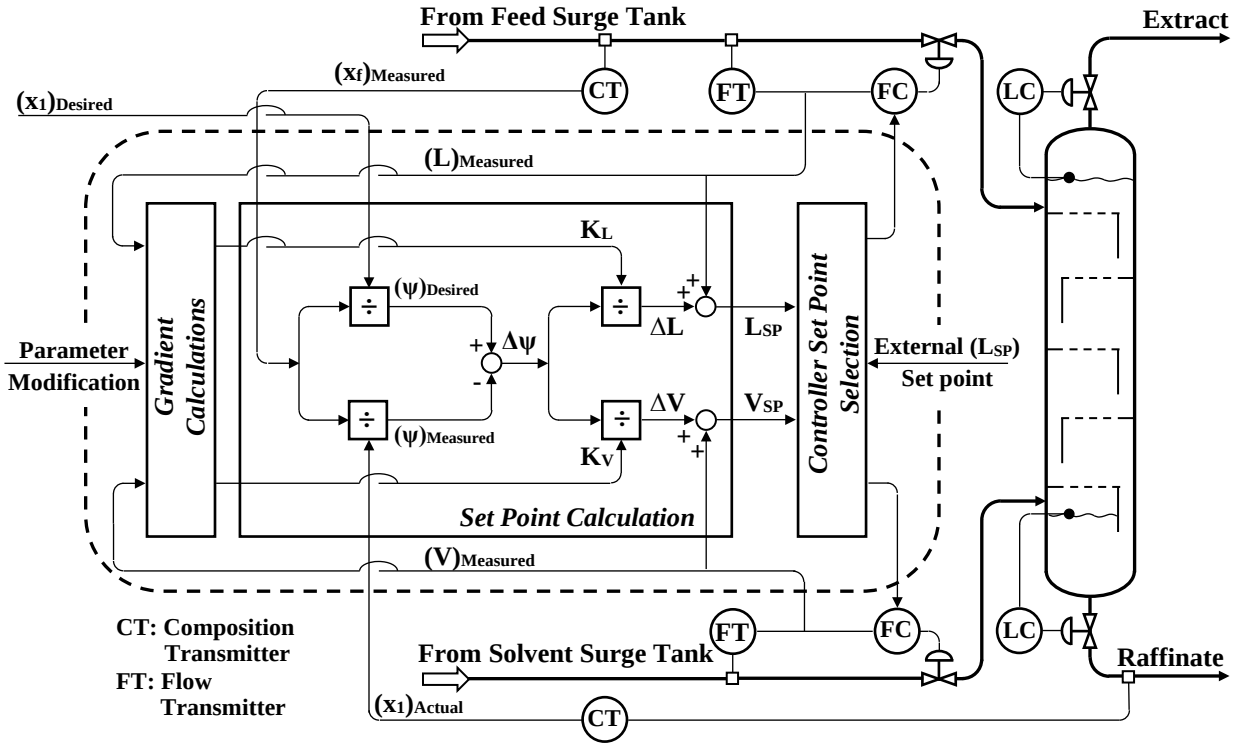

Figure (6) Block diagram of online steady state adaptive computer control scheme

The adaptive control computer consists of three sections. The first section computes the values of K_L and K_V expressed as polynomials in L and V. External inputs are used to introduce manually the numerical values of the polynomial coefficients for the system at hand. The two measured inputs to this section are the values of L and V while the outputs K_L and K_V are fed to the second section where the set points of the flow controllers are calculated. The external input to this section is the desired value of x_1 while the measured values of x_1 and x_f are used to calculate $(x_1/x_f)_A$. The deviation between the two values of ψ ($\Delta\psi = (x_1/x_f)_D - (x_1/x_f)_A$) is used to calculate the required changes in the set points for either the solvent (V_{SP}) or feed (L_{SP}) flow controllers, $\Delta V = \Delta\psi / K_v$ and $\Delta L = \Delta\psi / K_L$.

The third section of the control system deals with the selection of the set points of the two flow controllers. It either fixes the solvent rate at V_{max} or V_{min} while the feed rate is manipulated through the adaptive control computations or enables the manipulation of the solvent rate by the control computer while the feed rate flow controller set point is left free within its externally introduced range.

Considering the case when both flow rates lie within their operating range, the solvent rate is adjusted in order to produce the desired value of $(x_1/x_f)_D$ while the computed changes in the feed flow controller set point are ignored, despite variations in both L and x_f. In this case, the controller selector will keep $(\Delta L) = 0$ and thus $(\Delta V) = \Delta(x_1/x_f)/K_v$. When the solvent rate is kept constant at its maximum or minimum level, $(\Delta V) = 0$ and the required change in the feed rate is $(\Delta L) = \Delta(x_1/x_f)/K_L$.

The set points of the feed or solvent flow controllers are adjusted at suitable intervals depending on the size of the column till the required raffinate composition is obtained.

8. Conclusions

A simple steady state model based supervisory computer control scheme is suggested for un-agitated perforated plate extractive reactors subject to both measurable and un-measurable disturbances. For the nominal values of the design and physicochemical parameters, a previously developed model enables the prediction of the combination of solvent and feed flow rates required to achieve a given purification ratio of the raffinate.

The sensitivity of the purification ratio–phase flow rates response surface to disturbances associated with changes in the physicochemical parameters is illustrated. The computer control scheme takes care of such changes by correcting the computed model based flow rate perturbations on the basis of online comparison between the actual and desired purification ratios.
Under normal operating conditions, the suggested scheme provides for flexibility in feed flow rate and composition by adjustment of the solvent rate as long as both feed and solvent flow rates lie within the column hydrodynamic stability window. Whenever composition control calls for solvent rates, outside its allowable maximum and minimum range, manipulation of the feed rate rather than the solvent rate is included through a simple logic control function.

The effect of change in the physicochemical parameters on the steady state behaviour is to shift and distort the purification ratio-phase flow rate response surface. A model based adaptive control scheme is suggested to take care of such changes through an evolutionary mode of operation.

Appendix (A)

Fig. (A.1) outlines the ladder diagram of the programmable logic control function for selecting either the solvent rate or feed rate as the manipulated variable. When the computed solvent rate set point exceeds its maximum allowable value ($V>V_{max}$), contact (1) is switched on and two outputs will be produced. The first output (20) fixes the solvent flow rate at its maximum value and the second output (22) activates the computed feed flow rate set point overriding the external feed flow rate set point.

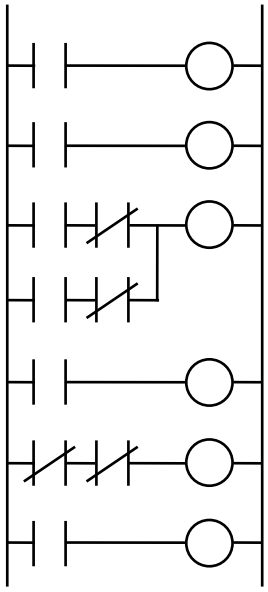

On the other hand if the calculated solvent flow rate is below its minimum allowable value ($V<V_{min}$) contact (2) is switched on and two other outputs will be produced.

Output (21) fixes the solvent flow rate at its minimum value, while output (22) activates the computed feed flow rate set point overriding the external feed flow rate set point.

When the solvent flow rate is within its allowable range, contacts (1) and (2) are switched off and output (24) is produced. In this case, the feed flow rate is left free within the externally defined constraints on its set point overriding the computed set point. The solvent rate set point will be modulated according to the value calculated by the control computer.

Nomenclature

a' : Interfacial area per unit volume of dispersed phase, $m^2\ m^{-3}$

A_a : Active perforated plate area, m^2

b : $1+e^{-\beta(1+\gamma)}+\frac{(1-e^{-\beta(1+\gamma)})}{g(1+\gamma)^2}+\frac{\beta}{g}\frac{\gamma}{(1+\gamma)}$

c : $e^{-\beta(1+\gamma)}+\frac{(1-e^{-\beta(1+\gamma)})}{g(1+\gamma)^2}+\frac{\beta}{g}\frac{\gamma}{(1+\gamma)}e^{-\beta(1+\gamma)}$

g : Extraction factor, L/mV

h : Effective stage contact height, m

k : Reaction rate constant, s^{-1}

K : Overall mass transfer coefficient, $m\ s^{-1}$

K_L : $(\partial\psi/\partial L)$

K_V : $(\partial\psi/\partial V)$

L : Volumetric flow rate of the continuous phase, $m^3\ s^{-1}$

m : Slope of the equilibrium relation

N : Number of actual plates

p_1, p_2 : Roots of the auxiliary quadratic equation, $p^2 - b\,p + c = 0$

V : Volumetric flow rate of the dispersed phase, $m^3\ s^{-1}$

x_1 : Solute concentration in the final raffinate, kmole m^{-3}

x_f : Solute concentration in the continuous phase feed, kmole m^{-3}

Greek Symbols

β : Dimensionless mass transfer parameter, $Ka'A_a\phi_D h/V$

ϕ_D : Dispersed phase holdup

γ : Reaction enhancement factor, k/Ka'

ψ : Purification ratio, x_1/x_f

Subscripts

A : Actual value

D : Desired value

max. : Maximum allowable

min. : Minimum allowable

ref. : At reference operating conditions

SP : Set point

References

Attarakih, M.M., Bart, H.J., Steinmetz, T., Dietzen, M., Faqir, N.M., 2008. LLECMOD: A bivariate population balance simulation tool for liquid-liquid extraction columns. The Open Chemical Engineering Journal. 2, 10-34.

Attarakih M., Abu-Khader, M., Bart, H.J., 2013. Modeling and dynamic analysis of a rotating disc contactor (RDC) extraction column using one primary and one secondary particle method (OPOSPM). Chem. Eng. Sci., 91, 180–196

Bart, H.J., 2002. Reactive extraction- status report on the simulation of stirred columns. Chem. Ing. Tech. 74 (3) 229-241.

Bemporad, A., Mosca, E., 1998. Fulfilling hard constraints in uncertain linear systems by reference managing. Automatica. 34(4) 451–461.

Chouai, A., Cabassud, M., LeLann, M.V., Courdon, C., Casamatta, G., 2000. Use of neural networks for liquid-liquid extraction column modeling: an experimental study, Chem. Eng. and Proc. 39, 171-180.

El Nashaie, S.S.E.H., El-Rifai, M.A., Abd El-Hakim, M.N., 1978. Effect of kinetic regime and axial dispersion on the dynamic response of counter flow extractive reactors. Chem. Eng. Sci. 33, 847-852.

El-Rifai, M.A., 1975. Composition dynamics in multi-mixer-settler extractive reaction batteries. Chem. Eng. Sci. 30(2) 79-87.

El-Rifai, M.A., El Nashaie, S.S.E.H., and Kafafi, A.A., 1977. Analysis of a countercurrent tallow-splitting column. Trans. Inst. Chem. Eng. 55, 59–63.

Ettouney, R.S., El-Rifai, M.A., Ghallab, A.O., 2007. Steady state modeling of perforated plate extraction columns. Chem. Eng. and Proc. 46, 713-720.

Ettouney, R.S., El-Rifai, M.A., 2011. Composition dynamics in perforated plate liquid extraction columns. Chem. Eng. Res. Des. 89(11) 2228-2235.

Ettouney, R.S., El-Rifai, M.A., 2012. Flow dynamics in perforated plate liquid extraction columns, Chem. Eng. Res. Des., 90 (11) 1417–1424

Hlawitschkah, M.W., Bart, H.J., 2012. CFD-mass transfer simulation of an RDC column. Comput. Aided Chem. Eng. 31, 920–924.

Mjalli, F.S., Abdel-Jabbar, N.M., Fletcher, J.P., 2005a. Modeling, simulation and control of a Scheibel liquid-liquid contactor, Part 2: Model-based control synthesis and design. Chem. Eng. and Proc. 44, 531-542.

Mjalli, F.S., Abdel-Jabbar, N.M., Fletcher, J.P., 2005b. Modeling, simulation, and control of a Scheibel liquid-liquid contractor: Part 1. Dynamic analysis and system identification. Chem. Eng. and Proc. 44, 541-553.

Morari, M., Lee, J.H., 1999. Model predictive control: past, present and future. Comput. Chem. Eng. 23, 667–682.

Najim, K., Le Lann, M.V., 1988. Multivariable learning control of an extractor. Chem. Eng. Sci. 43(7) 1539-1546.

Tang, X., Luo, G., Wang, J., 2004. A dynamic forward mixing model for evaluating the mass transfer performances of an extraction column. Chem. Eng. Sci. 59(21) 4457-4466.

Valentas, K.J., Amundson, A.R., 1966. Breakage and coalescence in dispersed phase systems. Ind. Chem. Eng. Fumdam. 5, 533-542.

Yadav, R.L., Patwardhan, A.W., 2009. CFD modeling of sieve and pulsed-sieve plate extraction columns. Chem. Eng. Res. Des. 87(1) 25-35.

A New Graphical Method for Pinch Analysis Applications: Energy Integration

Mamdouh A. Gadalla

British University in Egypt, Chemical Engineering Dept.
mamdouh.gadalla@bue.edu.eg

This research proposes a new graphical method for the analysis of heat recovery systems, applicable to both phases of grassroots and revamping. The new graphical method is based on plotting temperatures of process hot streams versus temperatures of process cold streams. A new graph is constructed for representing existing preheat trains. For a given preheat train, each existing exchanger is represented by a straight line, whose slope is proportional to the ratio of heat capacities and flows. Further, the length of each exchanger line is related to the heat flow transferred across this exchanger. This new graphical representation can easily identify exchangers-across-the-pinch, Network Pinch, pinching matches and improper placement of fuel consumption. Furthermore, such a graph can recognise promising modifications to improve the energy performance and hence less fuel and cooling water requirement. Graphs developed in this work can be used to analyse the energy performance of existing networks with respect to energy targets. They can also be used in junction with the background process to modify basic designs or existing network for better energy integration opportunities and minimum fuel demands.

Introduction

Pinch technology is an outstanding methodology for energy saving in processes where heating and cooling are characterising the processing operations. The concept

of Pinch Analysis is originally discovered and further developed in late 70s by Hohman (1971), Huang and Elshout (1976), Linnhoff et al. (1979, 1982) and Umeda et al. (1978). Yet it is evolving along the years and its applicability is broadening, mainly for saving material flows (El-Halwagi, 2012) and energy supplies. Pinch Analysis is found very popular and successful given the fact that it is conceptually simple and with impressive results, i.e. 10 to 35% in energy savings (NR Canada, 2003). The Pinch Analysis principles are set of rules, established using graphical representations such as Composite Curves, or by calculation-based methods known as the 'Problem Table Algorithm' (Linnhoff and Flower, 1978). Smith (2005) and Klemes (2013) provide a systematic procedure on how to construct Composite Curves for a given process, and outline the main features of such graphs. Maximum heat recovery is achieved within a given process, by complying with the principles of Pinch Analysis in the design for a given ΔT_{min}. Also in retrofit situation, the energy efficiency can be improved by removing violations to these principles.

Existing HENs are conventionally represented using grid diagrams. These diagrams are kind of sketches and can describe existing networks with details of connections but cannot interpret the principles of Pinch Analysis qualitatively nor quantify the energy inefficiencies particularly for very large HENs. In addition, the location of Network Pinch and Pinched Matches are not easy to detect using HEN grid diagrams, particularly for very complex networks, such as in refining processes. At the time that Composite Curves can describe fully new HEN designs, existing exchangers cannot be represented using such curves. It is valuable then if the existing network can be represented fully with its exact details of stream matches, temperatures and duties for better understanding to improve energy performances. It is also significant to graphically identify the locations of Network Pinch and limiting exchanger matches. Having represented an existing HEN with all associated details using new graphs, the Pinch Analysis principles and guidelines can be interpreted easier and thus energy improvement are obtained. Such graphs would be a key in performing revamping studies. The current research aims to tackle these previous observations and is to develop a new graphical tool featured with a new visualisation capability that will address such issues in existing methods.

A New Graphical Representation for Energy Analysis

The new graphical representation is obtained by plotting the temperatures of hot streams entering and leaving an exchanger unit versus those corresponding temperatures for cold streams. Thus, the y-axis is to represent the temperatures of all hot streams around exchangers whereas the x-axis is representing the corresponding cold streams temperatures, as demonstrated in Figure 1. Any process or utility hot stream can be represented by two horizontal lines on the diagram of Figure 1. The

upper horizontal line will represent the supply temperature of the stream, whereas the lower horizontal line will represent the target temperature. Similarly, cold process or utility streams will be represented through two vertical lines, one for the supply temperatures (to left side) and another for the target temperatures (to right side). The pinch temperatures of the process are plotted on the graph as a vertical line for the cold pinch temperature and a horizontal line for the hot pinch temperature. These two lines divide the graph into four distinct regions, left upper, right upper, left lower, right lower regions. Each region reflects the location of a group of exchanger matches within the heat exchanger network, as follows:

1. Left upper region: exchangers located in this region represent the matches exchanging or integrating heat between hot streams above the pinch with cold streams below the pinch.
2. Right upper region: exchangers located in this region represent the matches exchanging or integrating heat between hot streams above the pinch with cold streams above the pinch.
3. Left lower region: exchangers located in this region represent the matches exchanging or integrating heat between hot streams below the pinch with cold streams below the pinch.
4. Right lower region: exchangers located in this region represent the matches exchanging or integrating heat between hot streams below the pinch with cold streams above the pinch.

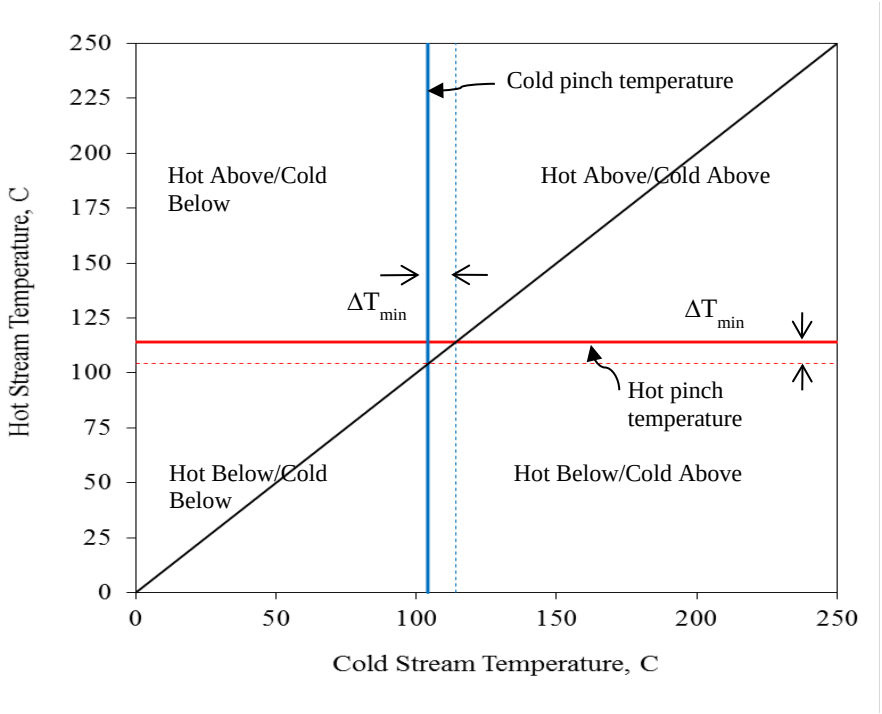

Figure 1: A new graphical representation for energy analysis

The new graphical representation shown in Figure 1 features the following:

5. Any point located inside the graph is defined by two temperature coordinates, i.e. (Tc, Th).
6. The minimum temperature approach difference appears twice, first with the vertical cold pinch temperature and then with the horizontal hot pinch temperature.
7. The diagonal line in the graph represents the case when hot stream temperatures approach cold stream temperatures or Th=Tc. Accordingly the diagonal divides the graph into two regions of heat integration, feasible energy integration above the diagonal, and infeasible energy integration below the diagonal. The infeasibility region below the diagonal is due to the fact that within this region any possible heat sources are colder than heat sinks. Therefore heat integration is thermodynamically impossible. This implies that all exchangers integrating heat must lie above the diagonal.
8. The 'Right Upper Region' is in energy balance with external hot utilities. Thus it is expected in this region that only heaters may appear.
9. The 'Left Lower Region' is similarly in energy balance with external cold utilities. Thus it is only allowed for energy efficient networks to have coolers within this region.

10. Exchanger matches located in the ‘Left Upper Region’ would transfer heat across the pinch. The heat integration of this region is still feasible, although it violates Pinch Analysis principles.
11. Energy integration or heat recovery for maximum energy efficiency will only take place through the exchangers in the two regions ‘Right Upper’ and ‘Left Lower’. Although the situation in many real plants of refining units or preheat trains is different that several exchanger matches are exchanging heat and are located within the region ‘Left Upper Region'. This last situation of poor design leads to inefficient heat integration or recovery in existing refineries and preheat trains. Thus considerable amounts of fuels and cooling utilities are consumed as a result of such a poor design. Therefore, these exchanger matches need particular consideration if the energy efficiency is to be maximised.
12. Coolers located in the Left Upper Region’ violate the Pinch Analysis principles. For this, the identification of such units is useful and would help in increasing the energy efficiency of an existing networks, i.e. heat loads on these coolers can be exploited for more energy integration. This feature may help in creating paths for heat integration. A path is linking a hot process stream and cold process stream with an exchanger unit at the presence of a relevant cooler and heater for these streams (Smith, 2005).
13. Exchanger matches touching the pinch temperatures from one point signify that these matches start or end heat integration between streams at the corresponding pinch temperatures, i.e. energy integration takes place at the pinch temperatures.

Consider a heat exchanger hx, transferring heat between a hot stream H and a cold stream C with a heat integration load of Q. The inlet temperature of hot and cold streams are Thin and Tcin respectively, while these streams leave the exchanger unit at Thout for the hot stream and Tcout for the cold stream. The hot stream has a mass flow rate of mh and a specific heat of Cph. On the other hand, the cold stream has a mass flow rate of mc and a heat capacity Cpc. Performing an energy balance on the given exchanger match results in:

$$Q = m_h \times C_{ph} \times \left(T_h^{in} - T_h^{out}\right) = m_h \times C_{ph} \times \Delta T_h \quad (1)$$

$$Q = m_c \times C_{pc} \times \left(T_c^{out} - T_c^{in}\right) = m_c \times C_{pc} \times \Delta T_c \quad (2)$$

If the heat capacities of hot and cold streams are considered constant across the range of temperatures, then Eq(1) and Eq(2) can be written as:

$$Q = \overline{CP}_h \times \left(T_h^{in} - T_h^{out}\right) = \overline{CP}_h \times \Delta T_h \quad (3)$$

$$Q = \overline{CP}_c \times \left(T_c^{out} - T_c^{in}\right) = \overline{CP}_{ch} \times \Delta T_c \quad (4)$$

where, $\overline{CP}_h$ is the mean heat capacity flow for the hot stream, and $\overline{CP}_c$ is the mean heat capacity flow for the cold stream. Dividing Eq(3) by Eq(4):

$$\overline{CP}_c/\overline{CP}_h = \Delta T_h/\Delta T_c \quad (5)$$

If the exchanger match is plotted on the new graphical representation as a straight line (with an arrow), then the line should start at the point (Tcout, Thin) and end at (Tcin, Thout); see Figure 2. The exchanger line is bounded by the temperatures of both the hot stream and cold stream. The hot temperatures could be the supply and target temperatures of the hot stream, or some of its intermediate temperatures. Likewise, the cold temperatures could represent the supply and target temperatures of the cold stream or its intermediate temperatures. Given the assumption of constant specific heat within the range of temperatures, exchangers are represented by straight lines. Still, variable thermal properties can be taken into account in the plot. The slope of the line representing exchangers is given by Eq(5), as the ratio between the heat capacity flows of cold stream to hot stream or the temperature difference of hot stream divided by that of the cold stream. Thus the vertical distance of the line is equivalent to ΔTh, while the horizontal distance is equivalent to ΔTc.

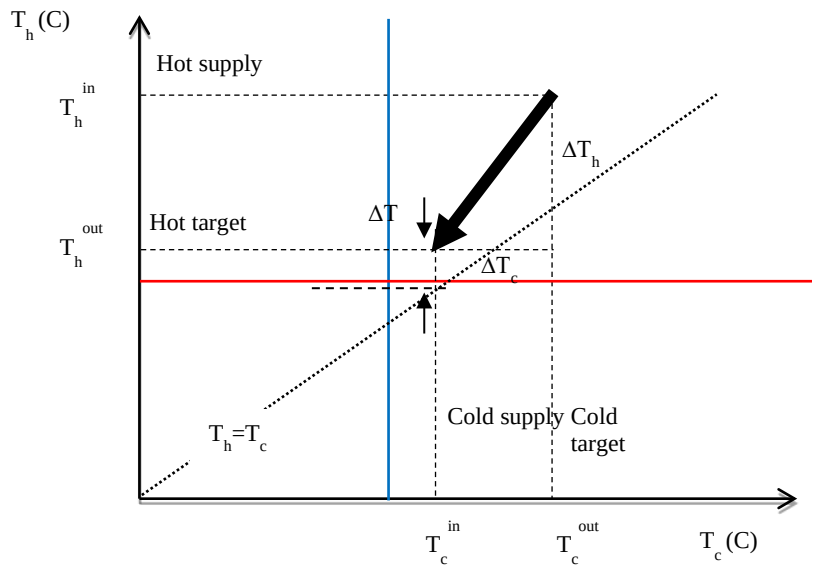

Figure 2: Representation of an exchanger match on the new graphical plot

A significant feature observed in Figure 2 is that the vertical distance between the straight line and the diagonal gives the temperature driving force profile across each exchanger (ΔT). The closet the exchanger line to the diagonal, the smallest the

temperature driving force the exchanger has. Then if the line is parallel to the diagonal, this implies a constant temperature driving force along the exchanger match. An exchanger match becomes a limiting for heat recovery as the line approaches the diagonal, and hence a decreased temperature driving force. This feature would help in identifying limiting exchanger matches for heat recovery by locating those matches with the smallest vertical distances to the diagonal, and hence temperature driving forces. The maximum heat recovery for an existing network is identified when exchanger matches tend to touch the diagonal in the graphical representation, where Th=Tc. Thus, these matches are pinching matches whenever heat recovery is maximised and a Network Pinch takes place.

An Illustrative Example – An Existing HEN

An existing heat exchanger network presented in previous work by Asante and Zhu (1997) is considered for the application of the new graphical representation. The case represents a real network of five exchanger units, as shown in Figure 3. The existing network has four hot streams and one cold streams. The existing network consumes hot utility and cold utility at the rate of 160 MW and 50 MW respectively.

The existing heat exchanger network is described using the new graphical method, and is demonstrated in Figure 4. A minimum temperature approach difference of 10 degrees Celsius is used in the new representation. Cold stream c1 is displayed by the vertical line at 100 ^{o}C for the supply temperature, and the vertical line at 190 ^{o}C for the target temperature. In the same way, hot stream h1 is represented through two horizontal lines at 160 ^{o}C and 120 ^{o}C for the supply and target temperatures respectively. Hot stream h4 is represented between the supply temperature of 200 ^{o}C and target temperature of 130 ^{o}C. For this ΔTmin, the pinch temperatures for the process streams are 150 and 140 ^{o}C for the hot and cold respectively; these pinch temperatures are easily obtained by using any traditional Pinch Analysis method such as given by Smith (2005). The energy targets for this process at ΔTmin=10 ^{o}C are 125 MW and 15 MW for hot energy and cold energy respectively. It is obvious that the existing network performs away from the energy targets. External hot utility is consumed by 28% more than energy target. This means that the real process excessively consumes a fuel oil or natural gas to provide the process heating. Therefore, a potential of fuel savings is available at the rate of 28%.
The existing heat exchanger network shown in Figure 4 can then easily be evaluated with respect to Pinch Analysis principles and energy targets, as follows:

(1) The heater E104 is appropriately placed in the region ‘Right Upper’.
(2) The two coolers E100 and E106 are partly inappropriately placed in the region ‘Left Upper’, where energy integration is to take place across the pinch.

(3) The exchanger matches E103 and E101 are integrating heat consistently with the Pinch design method. E103 is integrating energy from hot stream above the pinch to a cold stream above the pinch. Likewise, E101 is transferring the heat from hot stream below the pinch to a cold stream below the pinch. This means a Network Pinch may probably takes place at this exchanger match when energy integration is to be performed.

(4) The exchanger E101 is close to the diagonal, hence it is a potential limiting exchanger in energy saving projects.

(5) The exchanger E102 is integrating heat across the pinch, i.e. exchanging heat from above the pinch into below the pinch.

(6) For the current performance, there appears no pinching matches as none of the exchanger matches (represented by lines) touch the diagonal (ΔT_{min}=0 ºC) or the line corresponding to ΔT_{min}=10 ºC. On the contrary, there is still a positive vertical distance between the exchanger lines and the diagonal. This implies positive temperature driving forces and hence more potential for energy integration.

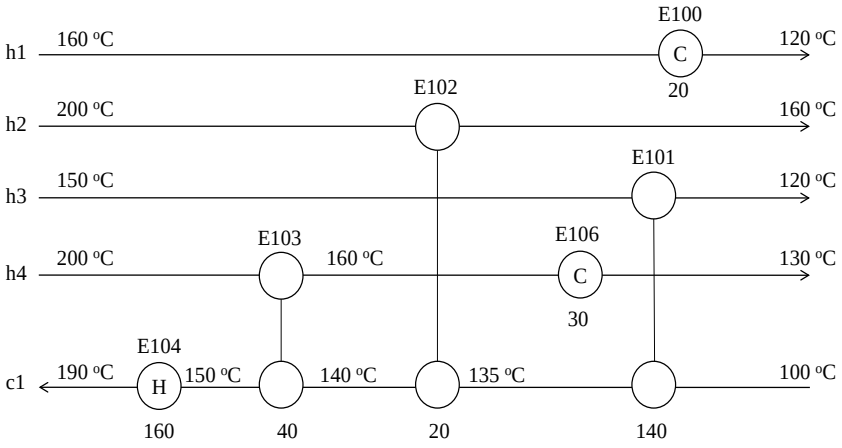

Figure 3: An existing heat exchanger network (numbers below exchangers refer to heat duties in MW)

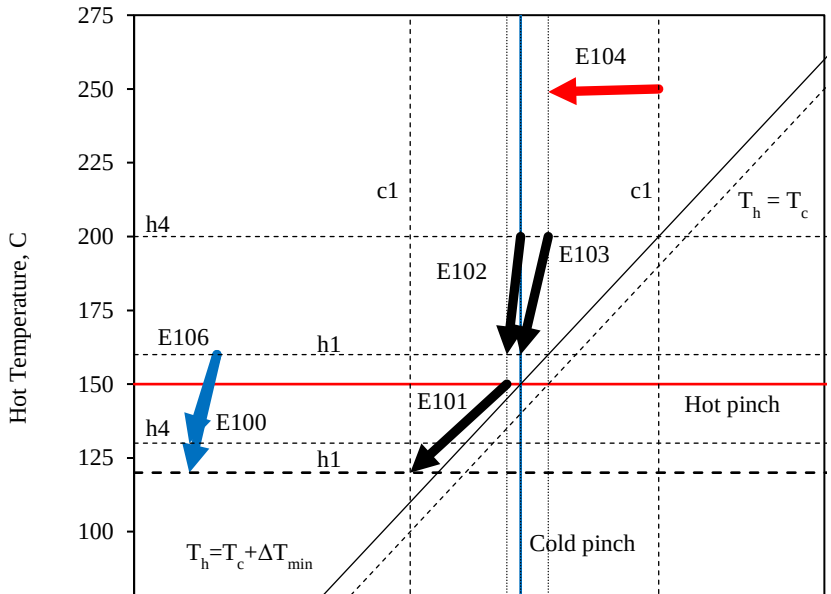

Figure 4: A new graphical representation for an existing HEN (small arrows refer to streams h1, h4 and c1)

Guided by the conclusions drawn from the graphical method of Figure 4, a modified HEN is proposed in Figure 5. The modifications proposed to the existing HEN are: modification #1; relocating the cooler E100 to recover more heat from the hot stream h1 through heating the cold stream c1rather than using cooling water, and modification #2; shifting the exchanger integrating heat across the pinch (E102) away from the region 'Left Upper' to the region 'Right Upper'. As a result of these modifications, more heat is integrated within the process (20 MW), and thus the heat load on the heater E104 decreases to 140 MW, compared with 160 MW for the existing network. This corresponds to a saving of 12.5% in the fuel consumption (or hot utility) and 40% for cooling water with the existing performance.

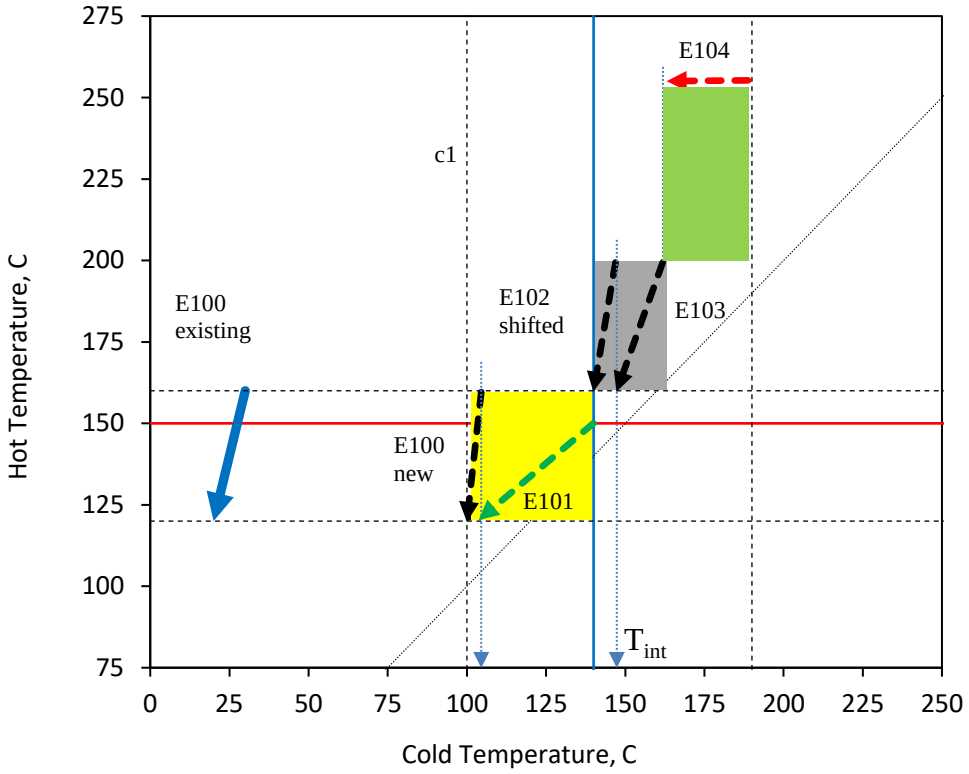

Figure 5: A graphical procedure for potential modifications for HEN revamping

Conclusions

In this work, a new graphical method has been developed to describe an existing heat exchanger network, including details of exchanger matches, heaters and coolers. Details of exchangers are plotted as temperatures of hot streams versus temperatures of cold streams. The new graphs can analyse and evaluate the performance of the existing HENs or preheat trains with respect to Pinch Analysis principles. Existing HEN energy inefficiencies are identified as a result of the performance analysis. Thus, the potential energy recovery is estimated through evaluating these inefficiencies quantitatively. The new graphical method is capable of proposing potential medications for better energy integration. The method also provides a systematic procedure, graphical-based by which potential modifications can be implemented. Various modification alternatives are also reached as a result of the new approach.

References

Asante N.D.K., Zhu X.X., 1997, An automated and interactive approach for heat exchanger network retrofit, Trans IChemE 75, 349

El-Halwagi M., 2012, Sustainable design through process integration. Elsevier, 1st ed, Oxford, UK

Klemeš J.J., 2013, Handbook of process integration (PI). Minimisation of energy and water use, waste and emissions. Woodhead Publishing Limited, 1st ed, Cambridge, UK

Linnhoff B., Mason D.R., Wardle I., 1979, Understanding heat exchanger networks, Comp Chem Eng 3, 295

Linnhoff B., Townsend D.W., Boland D., Hewitt G.F., Thomas B.E.A., Guy A.R., 1982, A User guide on process integration for the efficient use of energy. 1st ed, IChemE, UK

Linnhoff B., Flower J.R., Synthesis of heat exchanger networks: I. Systematic generation of energy optimal networks, AIChE J 24(4), 633–642

Hohman E.C., 1971, Optimum networks of heat exchange, PhD Thesis, University of Southern California, CA, USA

Huang F., Elshout R.V., 1976, Optimizing the heat recovery of crude units, Chem Eng Prog, 72:68

Natural Resources Canada, 2003, Pinch analysis: for the efficient use of energy, water & hydrogen. CANMET, ISBN: 0-662-34964-4, Catalogue # M39-96/2003E

Smith R., 2005, Chemical process design and integration. John Whiley & Sons Ltd, 1st ed, West Sussex, England

Umeda T., Itoh J., Shiroko K., 1978, Heat exchange system synthesis. Chem Eng Prog 74, 70